Chemistry - A European Journal 10.1002/chem.202001388

WILEY-VCH

FULL PAPER

The Underlying Chemistry to Formation of PO_2 Radicals from Organophosphorus Compounds - A Missing Puzzle Piece in the Flame Chemistry

Shuyu Liang[a,b], Patrick Hemberger*[c], Mathias Steglich[c], Pietro Simonetti[b], Joëlle Levalois-Grützmacher[a], Hansjörg Grützmacher[a] and Sabyasachi Gaan*[b]

Abstract: Reactive species such as $\cdot PO_2$ and HOPO are considered of upmost importance in flame inhibition and catalytic combustion processes of fuels. However, the underlying chemistry of their formation remains speculative due to the unavailability of suitable analytical techniques which can identify the transient species that lead to their formation. This study elucidates the reaction mechanisms of formation of phosphoryl species from dimethyl methyl phosphonate (DMMP) and dimethyl phosphoramidate (DMPR) under well-defined oxidative conditions. Photoelectron photoion coincidence techniques utilizing vacuum ultraviolet (VUV) synchrotron radiation were applied to isomer-selectively detect the elusive key intermediates and stable products. With the help of in-situ recorded spectral fingerprints different transient species, such as PO_2 and triplet O radicals, have been exclusively identified from their isomeric components, which helped piecing together the formation mechanisms of phosphoryl species under various conditions. It was found that $\cdot PO_2$ formation requires oxidative conditions above 1070 K. The combined presence of O_2 and H_2 led to significant changes in the decomposition chemistry of both model phosphorus compounds leading to the formation of $\cdot PO_2$. The reaction $\cdot PO + O_2 \rightarrow \cdot PO_2 + \cdot O\cdot$ was identified as the key step in the formation of $\cdot PO_2$. Interestingly, the presence of O_2 in DMPR thermolysis, suppresses formation of PN containing species. In a previous work, PN species were identified as the major species formed during the pyrolysis of DMPR. Thus, the findings of this study shed light onto decomposition pathways of organophosphorus compounds, which are beneficial for their fuel additive and fire suppressant applications.

Introduction

Increasing use of polymeric materials in every aspect of human life and stringent fire safety regulations are driving innovation in new flame retardants that are not only efficient but pose no toxicity concerns.[1] Since long organophosphorus compounds (OPCs) have been found to be important in combustion not only because they are proven to be efficient fire suppressants but also shown to be very useful in catalysis of hydrogen fuel in aircraft engine development.[2] The current discovery process of molecules or systems in both applications is tedious as it still has to follow an empirical or trial-and-error methodology. A profound understanding of the underlying chemistry of organophosphorus compounds in flame inhibition and combustion scenario is still missing but it should be the key to the future development of both flame retardants and fuel catalysis. Since decades, enormous efforts have been made to explore the working mechanism of few OPCs in both scenarios, wherein catalytic activities of phosphoryl species especially ·PO and HOPO were found to be responsible for either increasing the combustion efficiency of hydrogen fuel in a Scramjet or suppressing the hydrocarbon flame. Increasing importance of the use of phosphorus in combustion of fuels was demonstrated in a recent study, where phosphorus doped alumina has been utilized as solid support for the palladium-based catalyst for efficient methane combustion.[3]

A summary of well-characterized catalytic reactions of key phosphoryl species is outlined in e.q (1), (2) and (3).[4]

$$\cdot PO_2 + \cdot H \rightarrow HOPO \quad (1)$$
$$\cdot H + HOPO \rightarrow H_2 + \cdot PO_2 \quad (2)$$
$$\cdot OH + H_2 \rightarrow H_2O + \cdot H \quad (3)$$

Although these phosphoryl species have been found as the most important reactive intermediates for the efficient radical recombination activities in model OPC doped flames, their pathways of formation still lack robust experimental evidence.[5] Molecular beam technique coupled with mass spectrometry was used to study the OPC doped flame and the reaction pathways of key phosphoryl species were proposed by fitting the obtained MS data into the numerical models of hydrocarbon flames.[6] However, reaction intermediates leading to ·PO and $\cdot PO_2$ as well as the underlying mechanisms could not be unambiguously confirmed, which is due to the possible interference of dissociative ionization products and the corresponding isomeric masses. The mechanistic studies regarding thermal decomposition of OPC are

[a] Dr. S. Liang, Prof. Dr. J. Levalois-Grützmacher, Prof. Dr. H. Grützmacher
Laboratory of Inorganic Chemistry
ETH Zürich, Swiss Federal Institute of Technology
Vladimir-Prelog-Weg 1-5/10, Zürich, Switzerland
[b] Pietro Simonetti, Dr. S. Liang, Dr. S. Gaan
Additives and Chemistry, Advanced Fibers
Empa, Swiss Federal Laboratories for Materials Science
Lerchenfeldstrasse 5, Switzerland
E-mail: sabyasachi.gaan@empa.ch
[c] Dr. P. Hemberger, Dr. M. Steglich
Laboratory for Femtochemistry and Synchrotron Radiation
Paul Scherrer Institute
WSLA/115, Villigen-PSI, Switzerland
E-mail: patrick.hemberger@psi.ch

Supporting information for this article is given via a link at the end of the document.

restricted to only a few model compounds, while those studies for molecules that further include nitrogen element are mostly not accessible.[7]

In a recent work, vacuum ultraviolet (VUV) synchrotron radiation and imaging photoelectron photoion coincidence (iPEPICO) technique were combined to isomer-selectively track elusive phosphoryl species from the unimolecular decomposition process of OPCs in a hot micro reactor (depicted in Scheme 1) under inert conditions. It was found that the thermal decomposition of dimethyl methyl phosphonate ($(CH_3O)_2(CH_3)P=O$, DMMP) itself in an inert environment did not lead to $\cdot PO_2$ formation, instead it led to the production of phosphoryl radicals, ·PO. It is likely that the presence of oxygen during the thermal decomposition process is the key to its formation which is yet to be verified with appropriate experimental data.[8]

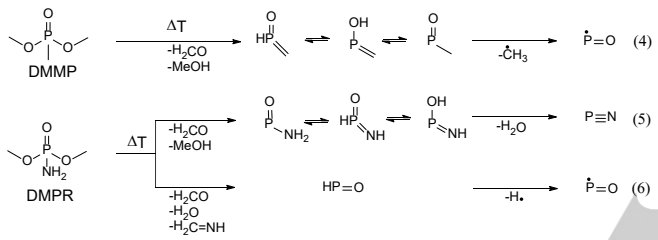

Scheme 1. Unimolecular decomposition pathway to afford ·PO and PN from dimethyl methyl phosphonate (DMMP) and dimethyl methyl phosphoramidate (DMPR).

In a subsequent study the thermal decomposition process of its analogue dimethyl phosphoramidate ($(CH_3O)_2(NH_2)P=O$, DMPR) was further investigated. Several pathways favorably yielding PN and a side reaction channel to PO radicals similar to that in DMMP were identified (see Scheme 1). [9] Again, no evidence regarding $\cdot PO_2$ formation from the DMPR decomposition could be established.

As $\cdot PO_2$ is considered important to the flame inhibition and the catalysis process in combustion, its formation pathways are of fundamental relevance to be studied. Thus, the focus of this study is to explore the reaction mechanisms of phosphoryl species in simulated combustion conditions, where $\cdot PO_2$ radicals are expected to be presented. Herein the pre-mixed hydrogen and oxygen mixture together with the chosen OPC molecule was passed through a resistively heated micro reactor, wherein a fully controlled gas inlet system was incorporated to create the combustion conditions and further explore the reaction mechanisms that lead to the formation of different phosphoryl species such as ·PO, $\cdot PO_2$ and HOPO. In the source chamber the reaction mixture leaving the reactor was expanded into the high-vacuum, where a molecular beam is formed and reactive intermediates are preserved. The skimmed molecular beam enters the photoelectron photoion coincidence (iPEPICO) spectrometer and gets ionized so that the formed electrons and ions are detected in delayed coincidences. The measured mass spectra at different temperatures and photoion mass-selected threshold photoelectron spectra (ms-TPES) were used to isomer-selectively detect stable products, as well as reactive intermediates. This technique has been proven to deliver reliable mechanistic insight in detection of elusive and reactive intermediates, in combustion[10], pyrolysis[11], discharge[12] and catalysis.[13]

Results and Discussion

Reaction of DMMP and DMPR in H_2 and O_2

The experimental design and measurement details are given in the experimental section. In brief, a series of time-of-flight mass spectra at 12 eV were measured at different reactor temperatures using argon as a carrier gas doped with H_2 and O_2 to investigate the underlying chemistry of DMMP ($(CH_3O)_2(CH_3)P=O$) and DMPR ($(CH_3O)_2(NH_2)P=O$), as depicted in Figure 1(a). Similar to the findings from our previous studies carried out under pyrolysis conditions, addition of 10% hydrogen in the reactor did not change the decomposition product distribution of neither DMMP nor DMPR (T until 1270 K). The evidence from the mass spectra and the associated threshold photoelectron spectra (ms-TPES) as fingerprints for each m/z are given in the supporting information Figure S1 and Table S1. In brief, the detected species at m/z 15, 30, 31, 32, 47, 62, 64 formed from DMMP + 10% H_2 can be assigned to methyl radical, formaldehyde, hydroxymethyl ion formed by dissociative ionization of methanol, ·PO, three isomers of $OPCH_3$ composition as well as HOPO, respectively.[9, 14] The analysis of the MS (Figure 1(b)) and ms-TPES of DMPR + 10% H_2 shows several identical spectral fingerprints as DMMP, but additionally at m/z 45, m/z 62, m/z 63 we find PN, P_2 and $PONH_2$ tautomers, again similar to the decomposition mechanisms at inert conditions.[8] The reaction pathways of DMMP and DMPR have been briefly summarized in Scheme 1. In both cases, DMMP and DMPR, PO_2 radicals (m/z 63) were absent in the hydrogen doped case. Upon addition of oxygen to the system the chemistry changes and details will be discussed as follow.

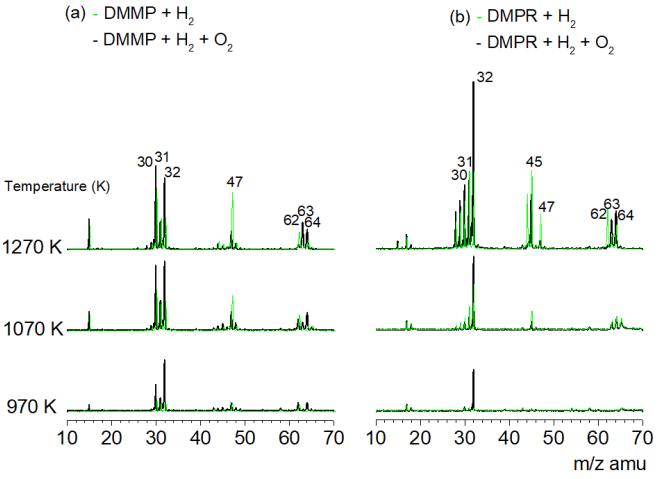

Figure 1. Temperature dependent photoionization mass spectra (TDMS) of DMMP (a) and DMPR (b) in H_2 and $H_2 + O_2$ from 298 to 1270 K taken at hv= 12 eV.

As depicted in Figure 1(a) for DMMP, introduction of 10% O_2 leads to new species presented at m/z 63 in the MS above 1070 K.[8] To confirm its chemical identity, the threshold photoelectron spectrum of m/z 63 was also recorded and is depicted in Figure 2. The ms-TPES shows a broad and unstructured band between 10.5 and 12 eV, which speaks for a large change in geometry upon ionization. Indeed, density functional theory suggests an increase of the O=P=O angle from 134 to 180° in agreement with removing an electron from the singly occupied molecular orbital located at the phosphorus. A Franck Condon simulation was also carried out, which is in very good agreement with the experimental ms-TPES spectrum and matches with the calculated adiabatic ionization energy of 10.75 eV (CBS-QB3) and clearly identifies the $\cdot PO_2$ radical as the major carrier of the signal at m/z 63.

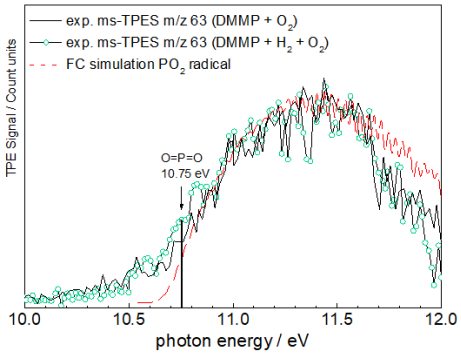

Figure 2. The mass selected threshold photoelectron spectra (TPES) for the species at m/z 63 in DMMP studies. A Franck Condon simulation of the $\cdot PO_2$ radical matches nicely with the experimental spectrum and clearly justifies the assignment.

Although a significant intensity change at m/z 63 was also noticeable within the temperature dependent mass spectra of DMPR upon O_2 addition, tracing the reasons behind is indeed challenging as $\cdot PO_2$ and the three $PONH_2$ isomers share the same nominal mass and ionization energies as found in our earlier study on the DMPR unimolecular pyrolysis process.[9] By simply comparing the two MS in Figure 1 one can notify the increased apparent abundance of species at m/z 63 above 1070 K upon addition of oxygen, which can either be attributed to faster production of $PONH_2$ tautomers or new isobaric (same nominal mass) species. To answer this question, we analyzed the threshold photoelectron spectra (see Figure 3) for the detected signal at m/z 63. The feature at 10.35 eV can be assigned to O=P-NH_2 isomer, thanks to the FC simulation also in agreement with our pyrolysis study.[9] The second band, however, starting to rise at around 10.7 eV, follows the same behavior as the PO_2 band, as recorded in the DMMP + H_2 + O_2 experiment. Thus, it is very likely that $\cdot PO_2$ contributes to the signal increase also upon oxidation of DMPR.

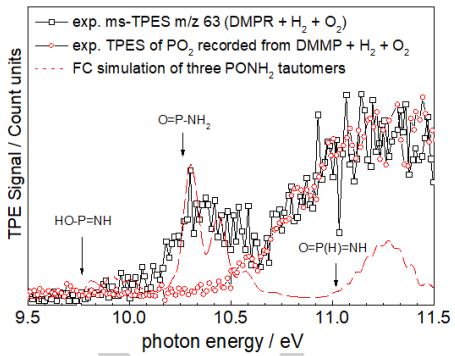

Figure 3. The TPES of species m/z 63 recorded at 1070 K upon oxidative thermolysis of DMPR, shows that beside PONH2 species also PO2 contributes to the spectrum.

Formation of $\cdot PO_2$ and the underlying chemistry upon O_2 addition

The thermal decomposition process of organophosphorus compounds in H_2 and O_2 involves unimolecular and bimolecular reactions. The unimolecular decomposition chemistry of DMMP and DMPR have been individually discussed in our previous studies.[8-9] Adding hydrogen to the reaction mixture did not change the products as compared to the pyrolysis measurements below 1270 K, as already discussed above. However, this changed upon adding oxygen:

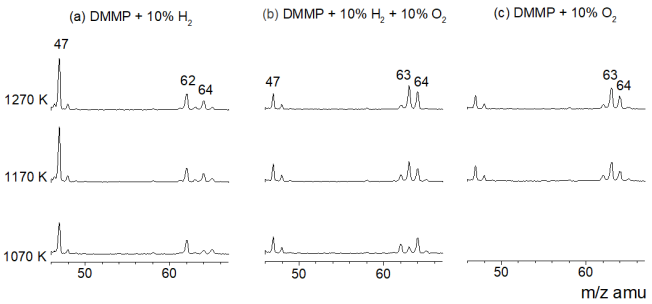

Figure 4. Detailed analysis on the temperature dependent photoionization mass spectra (TDMS) of DMMP (a,b,c) recorded at 12 eV.

To understand the details of underlying chemistry oxidation of phosphoryl species, additional time-of-flight MS were measured to observe the differences for the model compounds, as presented in Figure 4. It can be seen that the addition of 10% O_2 (b or c) into DMMP + H_2 (a) promoted the formation of $\cdot PO_2$ (m/z 63), and at same time the consumption of $\cdot PO$ (m/z 47) and its precursor $POCH_3$ (m/z 62) increased. It is thus believed that the intermediate $\cdot PO$ formed from the unimolecular decomposition process of DMMP (identified key reaction (7)[6b]) was oxidized to $\cdot PO_2$ by O_2. This can be further confirmed by a spectral identification of the oxygen triplet radical by-product ($\cdot O\cdot$, ^3P) involved in reaction (8). The confirmation of $\cdot O\cdot$ from the recorded spectra for m/z 16 is presented in Figure 5. In addition, the apparent abundance of HOPO also increased, which is in line with the known reactions (1), (2) given at the beginning of the article.

$$POCH_3 \rightarrow \cdot PO + \cdot CH_3 \quad (7)$$

$$\cdot PO + O_2 \rightarrow \cdot PO_2 + \cdot O \cdot \quad (8)$$

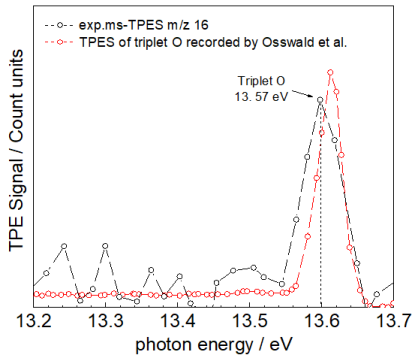

Figure 5. The TPES of species m/z 16 recorded at 1070 K upon oxidative thermolysis of DMPR which fits with the spectrum recorded by Osswald et al.[10b] The computed IE of triplet oxygen atom is 13.62 eV, which fully agrees with the ms-TPES spectra of species at m/z 16 recorded for the system that contains DMPR + H_2 + O_2.

As compared to its structural analogue DMMP, DMPR also tends to form $\cdot PO_2$ upon O_2 addition. As observed from Figure 6 (a) and (b), addition of 10% O_2 significantly increased the apparent abundance of isomers at m/z 63 ($\cdot PO_2$) and m/z 64 (HOPO) while reducing the abundance of ·PO (m/z 47) and P_2 (m/z 62, TPES given at SI). Following the same TPES identification for triplet O, it is evident that the intermediate ·PO (m/z 47) formed from the decomposition of DMPR was further oxidized to $\cdot PO_2$ (m/z 63) through the above-mentioned reaction (8). Meanwhile, P_2 (m/z 62), known as a bimolecular biproduct of the decomposition of DMPR, observed above 1270 K (Figure 6 d), also vanished and contributed to the $\cdot PO_2$ formation through reaction (9).

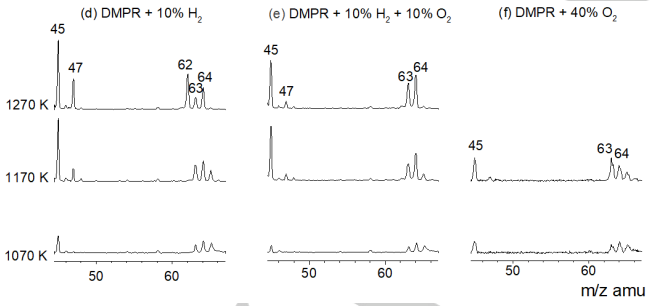

Figure 6. Detailed analysis on the temperature dependent photoionization mass spectra (TDMS) of DMPR (a,b,c) recorded at 12 eV.

$$P_2 + O_2 \rightarrow 2PO\cdot \quad (9)$$

Our previous work on unimolecular decomposition reactions of DMPR has outlined two major pathways leading to PN and a minor pathway leading to ·PO.[9] Therefore the observed signal reduction of PN (m/z 45) upon O_2 addition also deserves further attention (see Figure 6 (a) and (b)). This may be interpreted that the consumption of ·PO by O_2 has changed the equilibrium of the decomposition pathways to PN and that PN was further converted to ·PO and $\cdot PO_2$ via (10) and then (8). To support this argument, we tried introducing more O_2 at 1070K and 1170 K, which further shifted the equilibrium and indeed led to an instant signal suppression at m/z 45 (PN) in the MS in Figure 6 (f). The formation of $\cdot PO_2$ equilibrated further to afford increasing amount of HOPO, which is also noticeable in the MS for DMMP (Figure 4). Besides, the minor reaction (10) followed by (8) may also be involved for the PN consumption under oxidative conditions.

$$PN + O_2 \rightarrow \cdot PO + \cdot NO \quad (10)$$

In addition to the above discussed reaction pathways leading to the formation of $\cdot PO_2$ from both compounds, some flame studies [6b, 15] have suggested radical chain mechanisms that convert DMMP in combustion. Hydrogen abstraction reactions (·H, ·OH) that may lead to DMMP-H species (m/z 123), which subsequently lose formaldehyde to generate $PO(CH_3)(OCH_3)$ radical at m/z 93 or O_2PCH_3 (m/z 78) after a further demethylation are plausible. However, the associated products for this type of reaction were not directly observed in this study and the addition of H_2 and O_2 did not significantly change the product distribution pattern of the model compounds. More spectral details and calculated ionization energies (Table S2) for the species are provided in the supporting information SI. Figure S1, S6, S7 and S8 show additional mass spectra, but do not provide evidence for m/z 78, 93 and 123 originating from direct ionization of the phosphorus compounds.

Based on the detection of reactive intermediates in the high temperature chemistry of DMMP and DMPR molecules, it was found that upon addition of H_2 and O_2 the formation of $\cdot PO_2$ and HOPO, as the two major phosphoryl products, is enhanced. These conditions are comparable to a real combustion event, where these radicals are actively suppressing the formation of flame sustaining radicals such as ·OH. Such findings fill the missing puzzle pieces to understand the reaction mechanism of organophosphorus compounds in combustion process and will aid the development of novel organophosphorus compounds for applications in both fuel additive and fire suppressant domains.

Conclusion

Since long, the chemistry of flame inhibition of organophosphorus compounds and its characterization has been known to be complex and difficult due to the lack of spectroscopic tools to detect reactive species. In this study, the reactivities of two model organophosphorus candidates were systematically studied in a tubular micro-reactor applying an imaging photoelectron photoion coincidence (iPEPICO) technique with VUV synchrotron radiation. Thanks to photoion mass selected threshold photoelectron spectra we were able to unambiguously identify the isomeric composition for a given reaction process. This enabled us to untangle complex reaction mechanisms, especially for new organophosphorus flame retardants that carry nitrogen. We have studied the reaction mechanisms that produce $\cdot PO_2$ and HOPO from dimethyl methyl phosphonate (DMMP) and dimethyl phosphoramidate (DMPR). It was found that the underlying chemistry with H_2 and O_2 at elevated temperatures involves unimolecular decomposition of the OPC and bimolecular

reactions. DMMP undergoes sequential methanol, formaldehyde and methyl radical loss to yield ·PO radicals. As key finding of this study, we found that the PO radical is oxidized to yield $\cdot PO_2$ and atomic oxygen (^3P).

The availability of photoion mass-selected threshold photoelectron spectra as isomeric fingerprints enabled us to distinguish $PONH_2$ tautomers at m/z 63 from $\cdot PO_2$ in case of DMPR. Upon oxygen addition, the formation of $\cdot PO_2$ significantly suppresses the reactions that led to PN species.

The study on both compounds confirmed that $\cdot PO_2$ is only generated under oxidative conditions. Its generation was also associated with the production of additional HOPO in the reactor. Based on our study of DMMP and DMPR, it is concluded that the presence of both H_2 and O_2 has notably driven the formation process of $\cdot PO_2$ and HOPO as the two major phosphoryl reaction products above 1070 K, the temperature range of real combustion events. This study provides a fundamental insight into the formation mechanism of key phosphorus species responsible for either catalyzing or inhibiting the combustion chain reactions under different flame scenarios, which can aid in the future design of organophosphorus molecules for either fire suppressant or catalytic combustion applications.

Experimental Section

Dimethyl methyl phosphonate (>99.6%, 114 Pa, 25°C) was purchased from Sigma–Aldrich, Switzerland and distilled before use, while dimethyl phosphoramidate (>99.5%, 6.312 Pa, 91°C) was synthesized and purified following the procedure given in the literature.[9]

Synchrotron based experiments for underlying chemistry in details

The reaction products and the underlying chemistry of two model compounds in H_2 and O_2 were investigated at the VUV (X04DB) beamline at the Swiss Light Source at the Paul Scherrer Institute, Villigen, Switzerland.[16] The synchrotron light is generated from a bending magnet and directed into the spectrometer chamber of the PEPICO endstation using three optical elements. The monochromator is equipped with a 150 lmm^{-1} grating, providing a photon energy resolution of around 10 meV at 15.764 eV. Higher order radiation was suppressed using a differentially pumped gas filter and a Kr/Ne/Ar mixture. CRF-PEPICO spectrometer was utilized, which was recently developed by Sztaray et al.[17] This double imaging apparatus provides a higher mass resolution and velocity imaging for both ions and electrons as compared to the iPEPICO setup.[18]

To ensure consistent reaction condition for both compounds as mentioned in the introduction section, the flows of backing gas Ar and reacting gases H_2 and O_2 were controlled by three mass flow controllers and the same tubular sample reservoir equipped with a nozzle $\emptyset$=100 μm was used. The micro-tubular reactor consisted of a 1 mm iD SiC tubular reactor that can be resistively heated up to 1800 K under a total gas flow of 20 sccm ($Ar/H_2/O_2$). A Type C thermocouple was attached onto the SiC reactor between the two electrodes, which directly monitored the surface temperature. This allowed for measuring temperatures with ± 100 K accuracy.[19]

Dimethyl methyl phosphonate ($((CH_3O)_2(CH_3)P=O$) was seeded in Ar, H_2 and O_2 (0.39 bar) in a bubbler, which corresponds to a dilution of ≈ 0.3% (upper saturation limit) and expanded into the micro reactor. To provide stable flow conditions we waited a couple of minutes and recorded mass spectra to ensure stable signal. In order to achieve a similar concentration, dimethyl phosphoramidate ($((CH_3O)_2(NH_2)P=O$) was placed in the sample reservoir which was heated to 75°C by a copper block inside the source chamber. The residence time of the reaction mixture in the reactor was estimated to be within 100µs, based on the work by Guan et al.[20] The reaction mixture was expanded into high vacuum to obtain a continuous molecular beam. Only the central part of the molecular beam was skimmed (ø=2 mm) and enters the experimental chamber of the CRF-PEPICO. The beam intersects with tunable VUV light to generate ions and electrons, which were then extracted using a continuous, 120 or 240 $V \cdot cm^{-1}$ field. Photoelectrons were velocity-map imaged and detected by a fast delay-line detector (Roentdek) with a selected resolution of 5-10 meV.[21] The triggerless multi-start multi-stop detection scheme[22] was used, where the arrival of the electron is the time-zero for the photoion time-of-flight (TOF) analysis in the coincidence setup. TOF mass spectra were taken at different photon energies to help elucidate the most probable reaction pathways for both model compounds.

Photoion mass selected threshold photoelectron (ms-TPE) spectra and photoionization efficiency (PIE) curves were measured to disentangle the composition of different isomers. This was realized by using either the electrons arriving in the center of the detector[23] (threshold electrons) and then subtracting the hot-electron background, or using all kinetic energy electrons.

The Gaussian09[24] software suite was used to conduct the quantum chemical calculations, which applied the B3LYP functional and the 6-311++G(d,p) basis set to calculate equilibrium geometries and force constant matrixes as used in the Franck–Condon simulations (ezSpectrum or pgopher).[25] The line spectrum was subsequently convoluted with a Gaussian function for comparison with the experimental photoion mass-selected TPE spectrum. Reliable ionization energies for species assignment were calculated using the CBS-QB3 method.[26]

Acknowledgements

The measurements were carried out at the VUV beamline of the Swiss Light Source, Paul Scherrer Institute (PSI). Quantum chemical calculations were performed at Euler Cluster at ETH Zürich and using Merlin 5 at PSI. The authors are thankful to Mr. Ruohan Zhao, Mr. Thibeaut for the beamline supports, Mrs. Elisabeth Michel for her help for GC-MS measurement. The work was financially supported by the Swiss Federal Office for Energy (BFE Contract Numbers SI/501269-01).

Keywords: Organophosphorus Compounds • Flame Enhancer and inhibitor • Phosphorus intermediates • Mechanism • Synchrotron based Photoionization • Spectral Fingerprints

[1] M. M. Velencoso, A. Battig, J. C. Markwart, B. Schartel and F. R. Wurm, *Angew Chem Int Ed Engl* **2018**, *57*, 10450-10467.
[2] a) A. Twarowski, *Combustion and Flame* **1995**, *102*, 55-63; b) A. Twarowski, *Combustion and Flame* **1993**, *94*, 91-107; c) A. Twarowski, *Combustion and Flame* **1993**, *94*, 341-348.
[3] X. Chen, Y. Zheng, F. Huang, Y. Xiao, G. Cai, Y. Zhang, Y. Zheng and L. Jiang, *ACS Catalysis* **2018**, *8*, 11016-11028.
[4] a) J. Ströhle and T. Myhrvold, *Combustion and Flame* **2006**, *144*, 545-557; b) J. E. N. G. Siow and N. Laurendeau, *Combustion Science and Technology* **2002**, *174*, 91-116.
[5] a) F. Takahashi, V. R. Katta, G. T. Linteris and V. I. Babushok, *Proc Combust Inst* **2019**, *37*; b) O. P. Korobeinichev and T. A. Bolshova, *Combustion, Explosion, and Shock Waves* **2011**, *47*, 12-18.
[6] a) M. W. Beach, N. G. Rondan, R. D. Froese, B. B. Gerhart, J. G. Green, B. G. Stobby, A. G. Shmakov, V. M. Shvartsberg and O. P. Korobeinichev, *Polymer Degradation and Stability* **2008**, *93*, 1664-1673; b) J. H. Werner and T. A. Cool, *Combustion and Flame* **1999**, *117*, 78-98.
[7] a) F. Takahashi, V. Katta, G. Linteris and V. Babushok in *Numerical Simulations of Gas-Phase Interactions of Phosphorus-Containing Compounds with Cup-Burner Flames*, Eds.: K. Harada, K. Matsuyama, K. Himoto, Y. Nakamura and K. Wakatsuki), Springer Singapore, Singapore, **2017**, pp. 751-758; b) T. A. Bolshova, V. M. Shvartsberg, O. P. Korobeinichev and A. G. Shmakov, *Combustion Theory and Modelling* **2016**, *20*, 189-202; c) P. A. Glaude, H. J. Curran, W. J. Pitz and C. K. Westbrook, *Proceedings of the Combustion Institute* **2000**, *28*, 1749-1756.
[8] S. Liang, P. Hemberger, N. M. Neisius, A. Bodi, H. Grützmacher, J. Levalois-Grützmacher and S. Gaan, *Chemistry – A European Journal* **2015**, *21*, 1073-1080.
[9] S. Liang, P. Hemberger, J. Levalois-Grützmacher, H. Grützmacher and S. Gaan, *Chemistry – A European Journal* **2017**, *23*, 5595-5601.
[10] a) J. Krüger, G. A. Garcia, D. Felsmann, K. Moshammer, A. Lackner, A. Brockhinke, L. Nahon and K. Kohse-Höinghaus, *Physical Chemistry Chemical Physics* **2014**, *16*, 22791-22804; b) P. Oßwald, P. Hemberger, T. Bierkandt, E. Akyildiz, M. Köhler, A. Bodi, T. Gerber and T. Kasper, *Review of Scientific Instruments* **2014**, *85*, 025101.
[11] V. B. F. Custodis, P. Hemberger, Z. Ma and J. A. van Bokhoven, *The Journal of Physical Chemistry B* **2014**, *118*, 8524-8531.
[12] F. Holzmeier, M. Lang, I. Fischer, P. Hemberger, G. A. Garcia, X. Tang and J. C. Loison, *Physical Chemistry Chemical Physics* **2015**, *17*, 19507-19514.
[13] a) P. Hemberger, V. B. F. Custodis, A. Bodi, T. Gerber and J. A. van Bokhoven, *Nature Communications* **2017**, *8*, 15946; b) V. Paunović, P. Hemberger, A. Bodi, N. López and J. Pérez-Ramírez, *Nature Catalysis* **2018**, *1*, 363-370.
[14] S. Liang, P. Hemberger, N. M. Neisius, A. Bodi, H. Grutzmacher, J. Levalois-Grutzmacher and S. Gaan, *Chemistry* **2015**, *21*, 1073-1080.
[15] a) O. P. Korobeinichev, S. B. Ilyin, V. M. Shvartsberg and A. A. Chernov, *Combustion and Flame* **1999**, *118*, 718-726; b) O. P. Korobeinichev, S. B. Ilyin, T. A. Bolshova, V. M. Shvartsberg and A. A. Chernov, *Combustion and Flame* **2000**, *121*, 593-609.
[16] a) A. Bodi, M. Johnson, T. Gerber, Z. Gengeliczki, B. Sztáray and T. Baer, *Review of Scientific Instruments* **2009**, *80*, 034101; b) M. Johnson, A. Bodi, L. Schulz and T. Gerber, *Nuclear Instruments and Methods in Physics Research Section A: Accelerators, Spectrometers, Detectors and Associated Equipment* **2009**, *610*, 597-603.
[17] B. Sztaray, K. Voronova, K. G. Torma, K. J. Covert, A. Bodi, P. Hemberger, T. Gerber and D. L. Osborn, *J Chem Phys* **2017**, *147*, 013944.
[18] D. L. Osborn, C. C. Hayden, P. Hemberger, A. Bodi, K. Voronova and B. Sztaray, *J Chem Phys* **2016**, *145*, 164202.
[19] A. M. Scheer, C. Mukarakate, D. J. Robichaud, M. R. Nimlos and G. B. Ellison, *The Journal of Physical Chemistry A* **2011**, *115*, 13381-13389.
[20] Q. Guan, K. N. Urness, T. K. Ormond, D. E. David, G. Barney Ellison and J. W. Daily, *International Reviews in Physical Chemistry* **2014**, *33*, 447-487.
[21] B. J. Whitaker, ed., *Imaging in Molecular Dynamics*, Cambridge University Press, **2003**, p.
[22] A. Bodi, B. Sztáray, T. Baer, M. Johnson and T. Gerber, *Review of Scientific Instruments* **2007**, *78*, 084102.
[23] B. Sztáray and T. Baer, *Review of Scientific Instruments* **2003**, *74*, 3763-3768.
[24] M. J. Frisch, G. W. Trucks, H. B. Schlegel, G. E. Scuseria, M. A. Robb, J. R. Cheeseman, G. Scalmani, V. Barone, B. Mennucci, G. A. Petersson, H. Nakatsuji, M. Caricato, X. Li, H. P. Hratchian, A. F. Izmaylov, J. Bloino, G. Zheng, J. L. Sonnenberg, M. Hada, M. Ehara, K. Toyota, R. Fukuda, J. Hasegawa, M. Ishida, T. Nakajima, Y. Honda, O. Kitao, H. Nakai, T. Vreven, J. A. Montgomery, J. E. Peralta, F. Ogliaro, M. Bearpark, J. J. Heyd, E. Brothers, K. N. Kudin, V. N. Staroverov, R. Kobayashi, J. Normand, K. Raghavachari, A. Rendell, J. C. Burant, S. S. Iyengar, J. Tomasi, M. Cossi, N. Rega, J. M. Millam, M. Klene, J. E. Knox, J. B. Cross, V. Bakken, C. Adamo, J. Jaramillo, R. Gomperts, R. E. Stratmann, O. Yazyev, A. J. Austin, R. Cammi, C. Pomelli, J. W. Ochterski, R. L. Martin, K. Morokuma, V. G. Zakrzewski, G. A. Voth, P. Salvador, J. J. Dannenberg, S. Dapprich, A. D. Daniels, Farkas, J. B. Foresman, J. V. Ortiz, J. Cioslowski and D. J. Fox in *Gaussian 09, Revision B.01*, *Vol.* Wallingford CT, **2009**.
[25] a) A. Mozhayskiy and A. I. Krylov in *ezSpectrum* http://iopenshell.usc.edu/downloads, *Vol.* **2014**; b) C. M. Western in *PGOPHER, a Program for Simulating Rotational Structure*, *Vol.* http://pgopher.chm.bris.ac.uk, University of Bristol.
[26] a) J. A. Montgomery, M. J. Frisch, J. W. Ochterski and G. A. Petersson, *The Journal of Chemical Physics* **1999**, *110*, 2822-2827; b) J. A. Montgomery, M. J. Frisch, J. W. Ochterski and G. A. Petersson, *The Journal of Chemical Physics* **2000**, *112*, 6532-6542.

10.1002/chem.202001388

Table of Contents

Keywords: Organophosphorus Compounds • Flame Enhancer and inhibitor • Phosphorus intermediates • Mechanism • Synchrotron based Photoionization • Spectral Fingerprints